Biomaterials Science

COMMUNICATION

View Article Online
View Journal | View Issue

Cite this: *Biomater. Sci.*, 2020, **8**, 101

Received 29th June 2019,
Accepted 18th October 2019

DOI: 10.1039/c9bm01009b

rsc.li/biomaterials-science

Multiphasic *microgel-in-gel* materials to recapitulate cellular mesoenvironments *in vitro*†

Dejan Husman, ‡[a,b] Petra B. Welzel,‡[a] Steffen Vogler,[c] Laura J. Bray, [a,d] Nicole Träber,[a,e] Jens Friedrichs,[a] Vincent Körber,[a] Mikhail V. Tsurkan, [a] Uwe Freudenberg,[a] Julian Thiele [f] and Carsten Werner *[a,b,g]

Multiphasic *in vitro* models with cross-scale heterogeneity in matrix properties and/or cellular composition can reflect the structural and compositional complexity of living tissues more faithfully, thereby creating new options for pathobiology and drug development studies. Herein, a new class of tunable *microgel-in-gel* materials is reported that build on a versatile platform of multifunctional poly(ethylene glycol)-heparin gel types and integrates monodisperse, cell-laden microgels within cell-laden bulk hydrogel matrices. A novel microfluidic approach was developed to enable the high-throughput fabrication of microgels of *in situ* adjustable diameters, stiffness, degradability and biomolecular functionalization. By choosing structure and composition of the microgel and the bulk gel compartments independently, our *microgel-in-gel* arrangements provide cross-scale control over tissue-mimetic features and pave the way for culture systems with designed mesoenvironmental characteristics. The potentialities of the introduced approach are exemplarily shown by creating a reductionistic *in vitro* model of vascularized prostate cancer tissue.

[a]*Leibniz-Institut für Polymerforschung Dresden e.V. (IPF), Max Bergmann Center of Biomaterials Dresden (MBC), Hohe Str. 6, 01069 Dresden, Germany. E-mail: werner@ipfdd.de*

[b]*Technische Universität Dresden, Research Training Group "Nano- and Biotechniques for Electronic Device Packaging", Helmholtz Str. 18, 01069 Dresden, Germany*

[c]*Deutsches Zentrum für Neurodegenerative Erkrankungen (DZNE), Arnoldstr. 18, 01307 Dresden, Germany*

[d]*Queensland University of Technology (QUT), Institute of Health and Biomedical Innovation, 60 Musk Avenue, Kelvin Grove, 4059 Australia*

[e]*Technische Universität Dresden, Biotechnology Center (BIOTEC), Tatzberg 47/49, 01307 Dresden, Germany*

[f]*Leibniz-Institut für Polymerforschung Dresden e.V. (IPF), Department of Nanostructured Materials and Leibniz Research Cluster (LRC), Hohe Str. 6, 01069 Dresden, Germany*

[g]*Technische Universität Dresden, Center for Regenerative Therapies Dresden (CRTD), Tatzberg 47/49, 01307 Dresden, Germany*

†Electronic supplementary information (ESI) available: Experimental details, design and performance of the co-flow microfluidic device, cell-induced degradation of microbeads, monophasic 3D prostate cancer model, PC3 cells embedded into microbeads: spheroid formation and live/dead assay data. See DOI: 10.1039/c9bm01009b

‡These authors contributed equally to this work.

Tunable material platforms mimicking tissue-specific extracellular matrices (ECM) can be instrumental for regenerative therapies and for creating three-dimensional (3D) *in vitro* tissue and disease models. Various types of hydrogels were shown to be effective in recapitulating specific aspects of cell–matrix and cell–cell interactions.[1–12] However, homogeneous materials can not reflect the complexity of living tissues and are limited in supporting locally differing biomolecular and physical requirements of heterocellular cultures. Hydrogel materials with defined spatial distribution of cell-instructive properties as well as spatial separation of co-cultured cell populations produced by 3D printing,[13–18] photolithographic patterning,[19] microfluidics,[20] and other microfabrication techniques[21–23] were shown to be advantageous for reconstituting structural features of living tissues more closely. For instance, the provision of growth factors,[24] the spatial display of biological ligands,[20] and the mechanical heterogeneity of ECM[18] have been successfully mimicked with these approaches. However, a more faithful reconstitution of structural and functional features of living tissues by 3D *in vitro* models requires the combination of multiple functionalities *and* defined 3D architectures across scales.

Toward this aim, we herein present a new multiphasic biomaterials design approach (Fig. 1) that relies on integrating cell-laden spherical hydrogel microparticles (referred to as microgels) within cell-laden bulk hydrogel matrices to provide thoroughly tunable *microgel-in-gel* systems. Building on a recently developed platform of multifunctional glycosaminoglycan-based biohybrid hydrogels,[25] this approach allows for independently customizing the microgel and the bulk gel compartments with respect to cell-instructive matrix properties (stiffness, degradability, presentation of adhesion moieties and growth factors) and cellular composition. Moreover, it provides control over the spatial combination of the compartments (microenvironments), *i.e.* enables the design of *cellular mesoenvironments*[26] (Fig. 1). Micro- and mesoenvironmental parameters can be fine-tuned to reflect fundamental tissue properties in 3D culture. In particular, adjusting the microgel

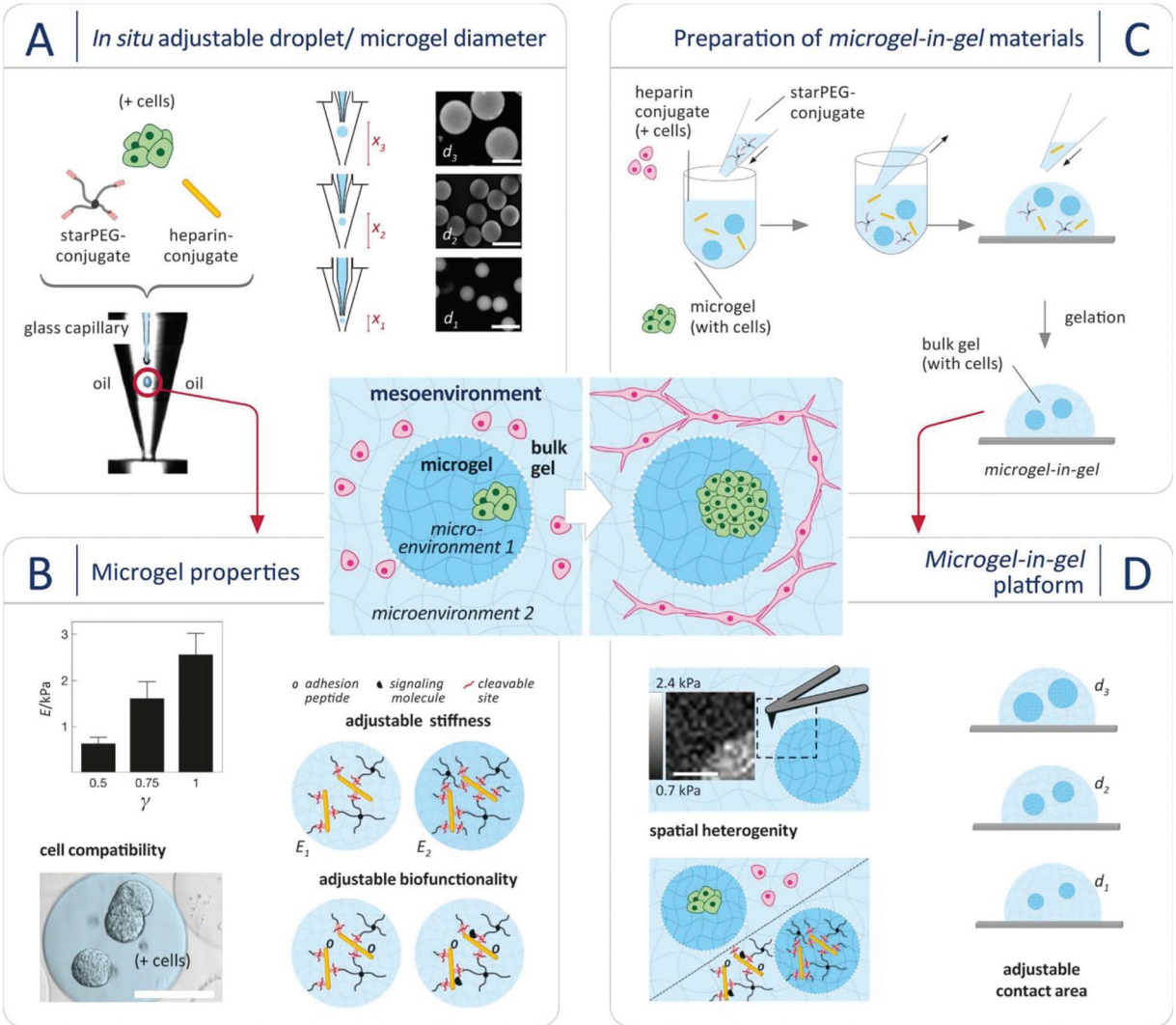

Fig. 1 Design of *microgel-in-gel* systems made of multifunctional poly(ethylene glycol)-heparin hydrogel types to recapitulate cellular mesoenvironments. Center: The systems allow for adjusting micro- and mesoenvironmental parameters to reflect fundamental tissue properties or direct the maturation of 3D cell assemblies. (A) Microgels with tunable diameter *d* can be easily produced from aqueous solutions of the starPEG- and the heparin conjugate (optional with cells) within the course of one experiment ("*in situ*") using a novel variant of droplet microfluidics. The approach relies on controlling the droplet diameter only by adjusting the position of the capillary *x* in a co-flow device (x_1 = 0.75 μm, x_2 = 1.5 μm, x_3 = 2.2 μm) at constant volumetric flow rates of disperse (0.5 mL h^{-1}) and continuous (216 mL h^{-1}) phase. Scale bars: 500 μm. (B) Microgel stiffness *E* (Young's modulus) is tunable by changing the molar starPEG to heparin ratio γ as determined by AFM-based nanoindentation. Biofunctionality of the microgels can be customized and cells can be embedded. Scale bar: 200 μm. (C) *Microgel-in-gel* systems of spatially gradated stiffness, biofunctionality and/or cellular composition were created by embedding starPEG-heparin microgels in starPEG-heparin bulk hydrogels. (D) A 100 μm × 100 μm color coded force map (AFM-based nano-indentation) of the interface between a microgel (γ = 1.0) embedded in a softer bulk hydrogel (γ = 0.63) demonstrated the successful formation of mechanically heterogeneous materials. Scale bar: 50 μm. Moreover, heterogeneity in biofunctionality and/or cellular composition, organization and function is possible. By adjusting the microgel diameter the extent of interaction across the microgel/bulk gel boundaries can be defined.

size obviously enables the graduation of interactions between the two engineered compartments (Fig. 1D). To exploit that option, a novel droplet microfluidics scheme was established to produce sets of monodisperse, cell-laden microgels of different sizes through crosslinking peptide-functionalized, four-armed poly(ethylene glycol) (hereafter: starPEG-conjugate or starPEG) and maleimide-functionalized heparin (hereafter: heparin-conjugate or heparin).[27] Second, *microgel-in-gel* systems of spatially gradated stiffness, biofunctionality and/or cellular composition were created by embedding starPEG-heparin microgels in starPEG-heparin bulk hydrogels with different composition and properties.

Finally, the methodology was exemplarily applied to mimic basic patterns of vascularized cancer tissue in a new format that overcomes limitations of 3D *in vitro* tissue models based on monophasic hydrogel materials: separately engineered hydrogel microenvironments, one supporting tumor spheroid formation of cancer cells and one supporting capillary

network formation of vascular endothelial cells, were combined in *microgel-in-gel* co-cultures to explore the *mesoenvironmental interplay* of the co-cultured cells.

Our material concept relies on the rational design of modular starPEG-heparin hydrogels[25,28] which uniquely allows the decoupling of biomolecular and biophysical matrix cues, creates powerful options for the biomimetic presentation of growth factors and enables the incorporation of adhesive peptide ligands and enzymatically degradable peptide crosslinkers as well as the precise adjustment of mechanical matrix stiffness (easily tuned by altering the molar starPEG to heparin ratio, γ).[29–32] Crosslinking of the pre-functionalized polymeric gel precursors (starPEG-conjugate and heparin-conjugate) by a rapid, cyto-compatible Michael-type addition reaction affords cell embedding under very mild conditions, avoiding exposure to UV light or temperature change.[7,27,33–35] To tailor droplets of polymer precursor solutions and microgels, respectively, in size, morphology (*e.g.* spherical, pancake-like or elongated) and compositional heterogeneity (*e.g.* Janus-like or core–shell), design features of microfluidic devices were to be optimized.[36–39] Rapid prototyping by combined photo- and soft lithography, supported by computational fluid dynamics (CFD) simulations, is the standard method of choice for screening the impact of design parameters and microchannel geometry. Yet, as droplet properties can be varied merely to a limited extend by changes in flow ratio and overall flow velocity of disperse and continuous phase given a defined microchannel diameter and droplet-forming nozzle (*e.g.* flow focusing or T-junction), each change in the microgel properties requires a new microfluidic device.[40] We therefore developed a novel variant of droplet microfluidics to effectively vary the microgel diameter d without changing the microfluidic device and even within the course of one experiment (*i.e.* "*in situ*"). The approach relies on controlling the droplet diameter only by adjusting the hydraulic diameter (Fig. S1, for details compare ESI†) at constant volumetric flow rates of disperse and continuous phase. For implementing this method, a co-flow type device was constructed from micro-machined polycarbonate blocks to form a cone-shaped channel for the continuous phase with a glass capillary in its centre for the aqueous phase. Due to the cone-formed channel, the hydraulic diameter D_H and thus the local flow velocity of the oil phase at the droplet-forming nozzle can be changed at constant oil volumetric flow rate by regulating the relative position of the glass capillary in flow direction (Fig. 1). This principle provides control over droplet diameters across a wide range (200–700 μm) by adjusting the capillary position without altering any other parameter (Fig. 1), as demonstrated in Fig. S2 (ESI†) for water-in-oil (w/o) droplets. For a given capillary position, the resulting (w/o) droplets were found to be monodisperse, with coefficients of variance (CV) of less than 4% for all sizes produced, which is in accordance with previous studies on co-flowing streams.[41] Applying our novel method, starPEG-heparin microgels were produced for the first time and in a wide size range from two-component mixtures of the reactive polymeric precursors as shown in Fig. 1: Using three different glass capillary positions at constant volumetric flow rates, monodisperse microgel batches with diameters of 200 μm, 400 μm, and 600 μm were obtained. By changing the molar ratio of the polymeric gel precursors starPEG-conjugate to heparin-conjugate (γ) in the reaction mixture, the Young's modulus of the microgels was tunable from 0.6 kPa–2.5 kPa (Fig. 1B) as confirmed by colloid probe AFM-based nanoindentation (compare ESI†). The determined values are comparable to reference bulk hydrogels of similar composition[27,33] and match the stiffness of soft tissues.[42] The uniformity of the Young's moduli of microgels from one batch confirmed the effective mixing and reactive network formation within the droplets, which is a challenge for two-component mixtures of reactive polymeric precursors.

Using the accordingly prepared starPEG-heparin microgels, *microgel-in-gel* systems were fabricated by incorporating sets of microgels into bulk gels of differing characteristics (Fig. 1C). For example, microgels with a molar starPEG to heparin ratio of $\gamma = 1$ were embedded within a hydrogel matrix of $\gamma = 0.63$. The resulting material was sliced with a vibratome (for details compare ESI†). The cross-sectional slices were probed with AFM-based nanoindentation, providing local differences in Young's Moduli and force-indentation maps (100 × 100 μm, Fig. 1D) displaying the dimensions, shapes and mechanical properties of embedded microgels. The functionality of both hydrogel phases, customized in stiffness by the molar ratio of starPEG to heparin (γ), was further adjusted by incorporation of cell-adhesion mediating (RGD)- as well as matrix metalloprotease (MMP)-sensitive peptide sequences. Similar to the bulk hydrogels,[7,27,33] microgels containing enzyme-sensitive linkers were found to be effectively reorganized by embedded cells: Fig. S3 (ESI†) illustrates the decrease in microgel stiffness over the course of 7 days culture from 1.3 to 0.5 kPa by incorporated prostate cancer (PC3) cells (1×10^6 PC3 cells per mL hydrogel).

A few other approaches using microgels incorporated in a hydrogel matrix for co-culture have been recently published.[43,44] Lee *et al.*[44] produced gelatin microgels of varied size utilizing a common PDMS flow-focusing junction that does, however, not allow for the *in situ* variation of droplet size as the device introduced in the present study. Compared to the gelatin-based co-cultures of Lee *et al.*, our starPEG-heparin hydrogel-based system does not only allow for tuning the physical properties of the different microenvironments, but also for the independent and liberal variation of their biomolecular properties. Therefore, we have been able to investigate the mesoenvironmental interplay of cell aggregates/assemblies, whereas Lee *et al.* explored the interaction of single cells only. Visser *et al.*[43] described an innovative in-air microfluidics methodology for high-throughput one-step printing of larger 3D biomaterials with modular architecture. In contrast to our approach, the applied set-up does not allow for combining cell assemblies, such as spheroids, in customized matrices at different time points, *i.e.* at different levels of maturation, as both hydrogel phases (microgels and surrounding matrix) are printed simultaneously.

To demonstrate the suitability of our novel *microgel-in-gel* platform for adjusting *cellular mesoenvironments* in tissue- or disease-specific ways, a previously established monophasic hydrogel-based 3D culture model of vascularized prostate cancer tumors[33] was translated into the *microgel-in-gel* co-culture format. Thereby, we aimed to overcome drawbacks of the monophasic model that will be discussed below. *In vivo*, new blood vessels are formed and sprout toward the tumor due to interactions between the cancer cells and endothelial cells. Hereby, the metabolic activities of tumors for further growth is supported, the invasion of cancer cells through the formed blood vessels for metastasis is enabled, and paracrine stimulations for cancer cells against apoptosis is facilitated.[21,45,46] Consequently, 3D *in vitro* models recapitulating the interaction between the cancer cells, capillary network-forming endothelial cells and matrix components can be instrumental to unravel the complex crosstalk underlying cancer growth and to develop and reliably test anti-cancer drugs. In the monophasic 3D prostate cancer model[33] mentioned above, human prostate cancer cells (PC3)[47] share one common starPEG-heparin hydrogel matrix with a capillary network-forming co-culture of human umbilical cord endothelial cells (HUVECs) and mesenchymal stromal cells (MSCs). The chosen properties of the utilized hydrogel matrix had to be a compromise between the requirements of the two different cell populations. In a delicate balance, the gel stiffness had to be adjusted to keep the incorporated preformed prostate cancer spheroids rounded, while allowing the HUVECs and MSCs to remodel the gel matrix to form capillary networks. As invasive cancer cell types, such as PC3 cells,

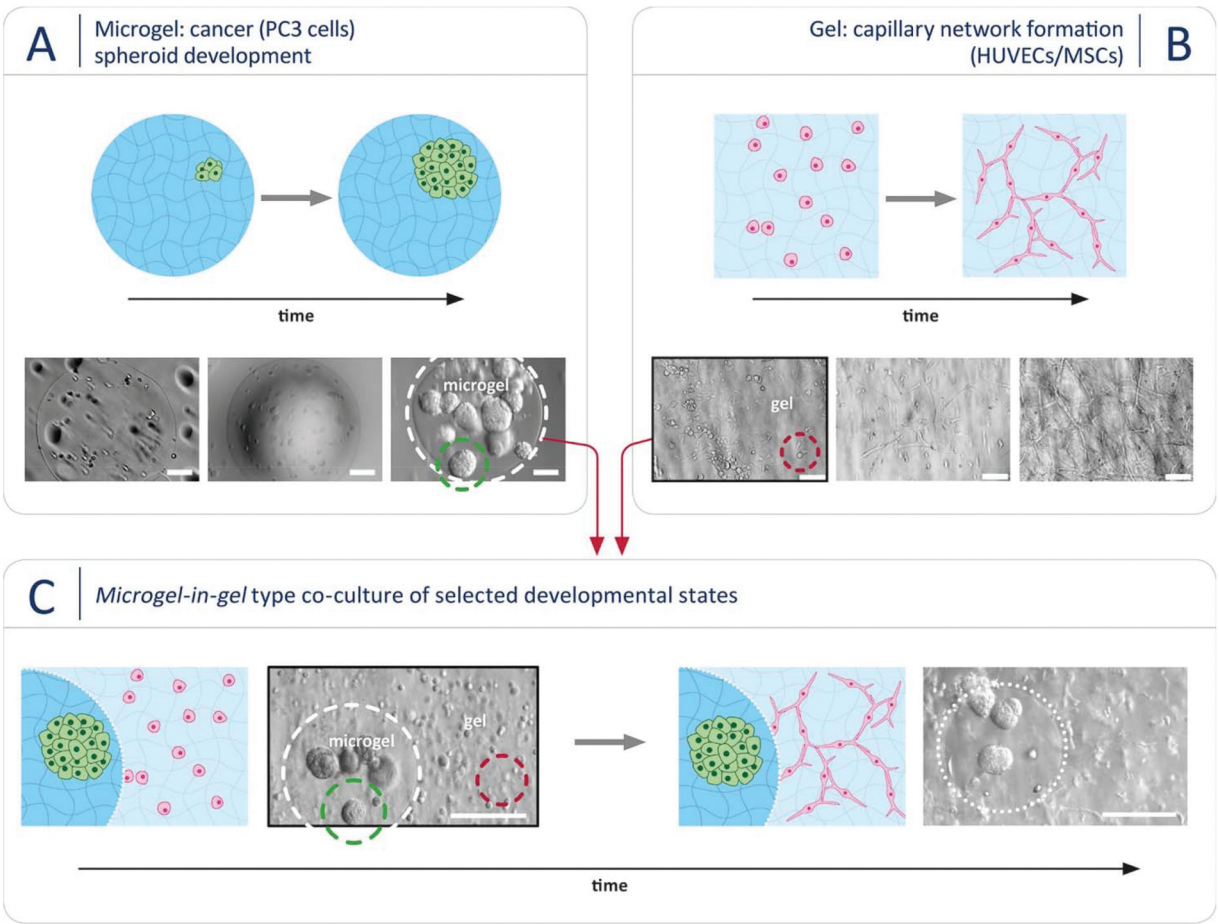

Fig. 2 3D *in vitro microgel-in-gel* prostate cancer model. Separately engineered starPEG-heparin hydrogel microenvironments, one supporting tumor spheroid formation of cancer cells (A) and one supporting capillary network formation of vascular endothelial cells (B), were combined in *microgel-in-gel* co-cultures (C) to explore the *mesoenvironmental interplay* of the co-cultured cells. (A) Prostate cancer cells (PC3) embedded in microgels crosslinked *via* MMP-sensitive peptide sequences (γ = 1) formed cancer spheroids in the course of 7 days; brightfield microscopy images at day 1, day 3, day 7. Scale bars: 100 μm. (B) Endothelial network formation from a HUVEC/MSC (10 : 1) co-culture in a bulk hydrogel. The material had a lower stiffness and additionally contained growth factors and adhesion ligands; brightfield microscopy images at day 0, day 1, day 7. Scale bars: 100 μm. (C) Both cell assemblies (spheroids and endothelial networks) can be combined to *microgel-in-gel* co-cultures at different time points, *i.e.* at different levels of maturation while keeping their microenvironment; as an example PC3 cells were grown into spheroids for 7 days within microgels which were subsequently embedded in HUVEC/MSC-laden bulk hydrogels; brightfield images of the *microgel-in-gel* co-cultures at day 0 (left) and day 2 (right). Scale bars: 200 μm.

better grow in stiffer microenvironments (most cancers result in a natural increase in ECM stiffness[48]), whereas soft hydrogels were required for capillary endothelial cell network formation,[7] PC3 spheroids had to be pre-formed separately, harvested and co-seeded together with HUVECs and MSCs in the soft hydrogel matrix. This procedure is not ideal, as it alters the cancer-specific ECM formed during natural spheroid formation. Moreover, the transplant of a pre-grown PC3 cell spheroid, once placed inside of the soft hydrogel matrix, will result in a spheroid that will disintegrate into (migratory) single cells, changing the cellular phenotype[33] as illustrated in Fig. S4 (ESI†). Additionally, PC3 cells quickly degrade the soft hydrogel leading to structural problems within the hydrogel culture. In contrast, our *microgel-in-gel* platform offers spatially segregated hydrogel compartments, which can be independently tuned to match the physical and biomolecular triggers of the desired cell organization and function. Using that option, we were growing tumor spheroids in a stiffer hydrogel matrix (microgel) surrounded by a soft hydrogel of functionally distinct properties (gel) suitable to support the co-culture of HUVECs and MSCs in the formation of a capillary endothelial cell network as exemplarily shown in Fig. 2. Due to this spatial (but connected) confinement of the two cell populations the reported system is beneficial: PC3 cells are grown in a stiffer, spheroid-supportive matrix in ways that allow for studying the paracrine effects of these cells on an environmental HUVEC/MSC network that is embedded in a softer matrix.

In the first step, prostate cancer cells (PC3; Deutsche Sammlung für Mikroorganismen und Zellkultur GmbH, DSMZ, Braunschweig, Germany) were mixed with a solution of pre-functionalized heparin and co-injected into the co-flow microfluidic device with a solution of peptide-functionalized starPEG (starPEG-conjugate, Fig. 1A); the resulting droplets cured to form microgels with embedded prostate cancer cells which developed into tumor spheroids during 7 days in culture (Fig. 2A). The microgels were produced with a starPEG to heparin ratio of $\gamma = 1$ to direct the growth of the PC3 cells into rounded spheroids by stiffer, tumor-like matrix properties[33] and contained MMP-cleavable peptide sequences to allow for cellular matrix remodeling. Live/dead staining indicated that encapsulation of the PC3 cells into starPEG-heparin microgels did not restrict cell survival and proliferation (Fig. S5, ESI†). In the second step, *microgel-in-gel* materials were prepared (Fig. 2C) by embedding microgels containing

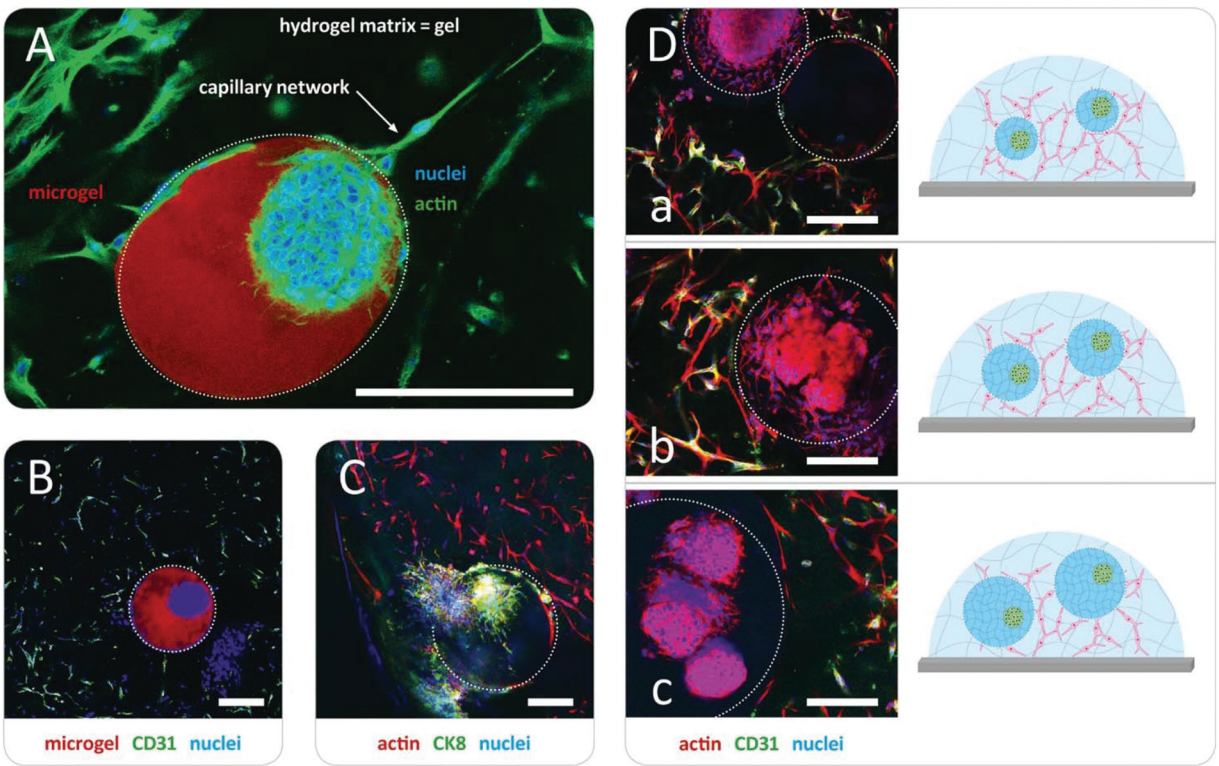

Fig. 3 Visualization of the 3D *in vitro microgel-in-gel* prostate cancer model by immunostaining/confocal microscopy 5 days after preparation. (A) Phalloidin staining of actin filaments (green) and Hoechst staining of nuclei (blue) highlights the prostate cancer spheroid embedded in the microgel with $\gamma = 1$ (within the dotted line, fluorescently labeled with Atto 610, red) as well as the capillary network (HUVECs/MSCs) in the surrounding hydrogel matrix ($\gamma = 0.63$). Scale bar: 250 μm. (B) HUVECs were identified by staining against CD31 (green). (C) The position of the cancer spheroid within the microgel was confirmed by staining against cytokeratin 8 (CK8). Scale bars (B and C): 200 μm. (D) Tuning the interfacial area between microgel and the surrounding hydrogel matrix (marked with dotted line) by using microgels with different diameter *d* (increasing *d* from (a) to (c); in (a) empty reference bead additionally embedded), enables manipulation of heterocellular and cell–matrix interactions; staining of actin filaments (red), nuclei (blue) and HUVECs (CD31, green/yellow) as mentioned above. Scale bars: 250 μm.

prostate cancer cells/spheroids after a defined pre-culture period (exemplarily shown for 7 days in Fig. 2A) together with suspended HUVECs (isolated from umbilical veins as previously described[49]) and MSCs (derived from healthy volunteer donors after informed consent. The use of surplus bone marrow cells for MSC generation was approved by the ethics committee of the Technical University Dresden (Ethics approval ID: EK127042009). Bone marrow-derived MSCs were isolated as previously described[50]) into a significantly softer bulk hydrogel matrix (gel). In the given example, this gel matrix (Fig. 2B) was formed with a lower molar starPEG to heparin ratio (γ = 0.63) and contained not only MMP-cleavable peptide sequences, but also covalently attached adhesion ligand peptides as well as a combination of pro-angiogenic growth factors at concentrations previously shown to effectively support angiogenesis (vascular endothelial growth factor (VEGF), stromal cell derived factor (SDF-1), and basic fibroblast growth factor (FGF-2)).[7,33] After 5 days, the *microgel-in-gel* culture resulted in vascularized matrix-embedded prostate cancer spheroids (Fig. 2C) and was thoroughly characterized by immunostaining/confocal laser scanning microscopy (CLSM) to confirm the established structures and identify the cellular components within the two distinct hydrogel compartments (Fig. 3A, B and C). The spatially resolved microtissue structures were found to be morphologically accurate, reflecting the *in vivo* architecture better than dual layer approaches with spatially restricted cancer and vascular cells.[51,52]

As a particular advantage of the approach, our *microgel-in-gel* cancer tissue model permits the defined recapitulation of different stages of tumor development *in vivo*. For that purpose, the culture format allows for combining cell assemblies, such as spheroids, in their customized matrices at different time points, *i.e.* at different levels of maturation (Fig. 2). Moreover in contrast to dual layer models,[51,52] the interfacial area and cross boundary interactions between the prostate cancer cell containing microgels and the surrounding bulk gel matrices containing capillary endothelial cell networks can be easily and systematically varied by the choice of the microgel size (Fig. 1D and 3D).

Applications of the introduced starPEG-heparin *microgel-in-gel* materials can benefit from the broad range of previously explored hydrogel variants with distinct growth factor signaling, adhesion ligand presentation, susceptibility for enzymatic cleavage, and stiffness. For example, *microgel-in-gel* materials with gradated mechanical properties of the two hydrogel phases can be used to target stiffness-dependent phenotypes of embedded PC3 cells under otherwise constant conditions: while spheroids (Fig. 2 and 3) were obtained in stiffer microgels, the same cell type appeared more migratory in the surrounding softer hydrogel matrix (Fig. 3C). Independently varying all the above-mentioned matrix properties within the distinct hydrogel phases of our *microgel-in-gel* materials offers unprecedented options for the identification of their relevance, *e.g.* in tumor progression, clearly going beyond the previously reported single parameter variations of stiffness[53,54] or density.[55] However, for detailed biological investigations the novel technology needs further optimization depending on the particular question of interest. For instance, exact control over the spatial arrangement of the cancer spheroids within the microgels is so far limited.

Conclusions

In summary, a powerful novel microfluidic technology was established for creating customized starPEG-heparin microgels that enabled the formation of *microgel-in-gel* materials containing differently cell-instructive and cell-laden hydrogel types. To demonstrate the potential of our modular design approach, a 3D prostate cancer tissue *in vitro* model was developed. In this example system, control over mesoenvironmental parameters – cancer stroma thickness, cancer spheroid size as well as microvasculature structure and density – provides unprecedented options for examining the tumor-stroma cross-talk during the early stages of tumor angiogenesis. We anticipate the approach will become instrumental for studying various further aspects of cancer biology, including invasion/metastasis, and tumor interactions with the endothelium, at high levels of precision *in vitro*. Beyond that, our introduced *microgel-in-gel* platform is expected to advance various demanding co- and organoid culture schemes, paving the way for an array of more realistic tissue and disease models.

Conflicts of interest

There are no conflicts to declare.

Acknowledgements

This research was supported by the DFG (Research Training Group "Nano- and Biotechniques for Electronic Device Packaging"). L. J. B. was supported by an Endeavour Fellowship as part of the Australia Awards program. MSCs were kindly gifted by Prof. Martin Bornhäuser (Universitätsklinikum Dresden). J. T. thanks the Federal Ministry of Education and Research (BMBF, "Biotechnologie2020+ Strukturvorhaben: Leibniz Research Cluster, 031A360C), and the DFG (Research Training Group "Hydrogel-based Microsystems" and TH 2037/1).

References

1 N. A. Peppas, J. Z. Hilt, A. Khademhosseini and R. Langer, *Adv. Mater.*, 2006, **18**, 1345–1360.
2 N. Huebsch and D. J. Mooney, *Nature*, 2009, **462**, 426–432.
3 E. S. Place, N. D. Evans and M. M. Stevens, *Nat. Mater.*, 2009, **8**, 457–470.
4 M. P. Lutolf and J. A. Hubbell, *Nat. Biotechnol.*, 2005, **23**, 47–55.

5 K. Y. Lee and D. J. Mooney, *Chem. Rev.*, 2001, **101**, 1869–1880.
6 E. González-Díaz and S. Varghese, *Gels*, 2016, **2**, 20.
7 K. Chwalek, M. V. Tsurkan, U. Freudenberg and C. Werner, *Sci. Rep.*, 2014, **4**, 8.
8 K. Chwalek, L. J. Bray and C. Werner, *Adv. Drug Delivery Rev.*, 2014, **79–80**, 30–39.
9 A. V. Taubenberger, L. J. Bray, B. Haller, A. Shaposhnykov, M. Binner, U. Freudenberg, J. Guck and C. Werner, *Acta Biomater.*, 2016, **36**, 73–85.
10 H. M. Weber, M. V. Tsurkan, V. Magno, U. Freudenberg and C. Werner, *Acta Biomater.*, 2017, **57**, 59–69.
11 M. Nowak, U. Freudenberg, M. V. Tsurkan, C. Werner and K. R. Levental, *Biomaterials*, 2017, **112**, 20–30.
12 C.-Y. Liaw, S. Ji and M. Guvendiren, *Adv. Healthcare Mater.*, 2018, **7**, 1701165.
13 Y. Yang, X. Song, X. Li, Z. Chen, C. Zhou, Q. Zhou and Y. Chen, *Adv. Mater.*, 2018, **30**, 1706539.
14 A. Nadernezhad, N. Khani, G. A. Skvortsov, B. Toprakhisar, E. Bakirci, Y. Menceloglu, S. Unal and B. Koc, *Sci. Rep.*, 2016, **6**, 33178.
15 T. Jiang, J. G. Munguia-Lopez, S. Flores-Torres, J. Grant, S. Vijayakumar, A. D. Leon-Rodriguez and J. M. Kinsella, *Sci. Rep.*, 2017, **7**, 4575.
16 K. Pataky, T. Braschler, A. Negro, P. Renaud, M. P. Lutolf and J. Brugger, *Adv. Mater.*, 2012, **24**, 391–396.
17 D. B. Kolesky, R. L. Truby, A. S. Gladman, T. A. Busbee, K. A. Homan and J. A. Lewis, *Adv. Mater.*, 2014, **26**, 3124–3130.
18 L. A. Hockaday, K. H. Kang, N. W. Colangelo, P. Y. C. Cheung, B. Duan, E. Malone, J. Wu, L. N. Girardi, L. J. Bonassar, H. Lipson, C. C. Chu and J. T. Butcher, *Biofabrication*, 2012, **4**, 035005.
19 C. A. DeForest and K. S. Anseth, *Angew. Chem.*, 2012, **124**, 1852–1855.
20 S. Kobel and M. P. Lutolf, *Curr. Opin. Biotechnol.*, 2011, **22**, 690–697.
21 W. Lee and J. Park, *Adv. Mater.*, 2012, **24**, 5339–5344.
22 M. P. Lutolf, P. M. Gilbert and H. M. Blau, *Nature*, 2009, **462**, 433.
23 N. J. S. Darling, E. Sideris, N. Hamada, S. T. Carmichael and T. Segura, *Adv. Sci.*, 2018, **8**, 1801046.
24 F. Han, F. Zhou, X. Yang, J. Zhao, Y. Zhao and X. Yuan, *J. Biomed. Mater. Res., Part B*, 2015, **103**, 1344–1353.
25 U. Freudenberg, Y. K. Liang, K. L. Kiick and C. Werner, *Adv. Mater.*, 2016, **28**, 8861–8891.
26 The term *mesoenvironment* (meso – from the Greek word 'intermediate') is introduced here to highlight the fact that adjacent cellular microenvironments with discrete characteristics give rise to heterocellular and cell-matrix interactions across spatial scales.
27 M. V. Tsurkan, K. Chwalek, S. Prokoph, A. Zieris, K. R. Levental, U. Freudenberg and C. Werner, *Adv. Mater.*, 2013, **25**, 2606–2610.
28 U. Freudenberg, J. U. Sommer, K. R. Levental, P. B. Welzel, A. Zieris, K. Chwalek, K. Schneider, S. Prokoph, M. Prewitz, R. Dockhorn and C. Werner, *Adv. Funct. Mater.*, 2012, **22**, 1391–1398.
29 K. Chwalek, K. R. Levental, M. V. Tsurkan, A. Zieris, U. Freudenberg and C. Werner, *Biomaterials*, 2011, **32**, 9649–9657.
30 U. Freudenberg, A. Zieris, K. Chwalek, M. V. Tsurkan, M. F. Maitz, P. Atallah, K. R. Levental, S. A. Eming and C. Werner, *J. Controlled Release*, 2015, **220**, 79–88.
31 S. Prokoph, E. Chavakis, K. R. Levental, A. Zieris, U. Freudenberg, S. Dimmeler and C. Werner, *Biomaterials*, 2012, **33**, 4792–4800.
32 L. Schirmer, P. Atallah, C. Werner and U. Freudenberg, *Adv. Healthcare Mater.*, 2016, **5**, 3157–3164.
33 L. J. Bray, M. Binner, A. Holzheu, J. Friedrichs, U. Freudenberg, D. W. Hutmacher and C. Werner, *Biomaterials*, 2015, **53**, 609–620.
34 L. J. Bray, M. Binner, Y. Körner, M. von Bonin, M. Bornhäuser and C. Werner, *Haematologica*, 2017, **102**, 1215–1226.
35 L. J. Bray, C. Secker, B. Murekatete, J. Sievers, M. Binner, P. B. Welzel and C. Werner, *Cancers*, 2018, **10**, 292.
36 L. Zhang, K. Chen, H. Zhang, B. Pang, C.-H. Choi, A. S. Mao, H. Liao, S. Utech, D. J. Mooney, H. Wang and D. A. Weitz, *Small*, 2018, **14**, 1702955.
37 A. S. Mao, J.-W. Shin, S. Utech, H. Wang, O. Uzun, W. Li, M. Cooper, Y. Hu, L. Zhang, D. A. Weitz and D. J. Mooney, *Nat. Mater.*, 2016, **16**, 236–243.
38 Y. Hu, A. S. Mao, R. M. Desai, H. Wang, D. A. Weitz and D. J. Mooney, *Lab Chip*, 2017, **17**, 2481–2490.
39 C.-H. Choi, H. Wang, H. Lee, J. H. Kim, L. Zhang, A. Mao, D. J. Mooney and D. A. Weitz, *Lab Chip*, 2016, **16**, 1549–1555.
40 S. Xu, Z. Nie, M. Seo, P. Lewis, E. Kumacheva, H. A. Stone, P. Garstecki, D. B. Weibel, I. Gitlin and G. M. Whitesides, *Angew. Chem., Int. Ed.*, 2005, **44**, 724–728.
41 G. F. Christopher and S. L. Anna, *J. Phys. D: Appl. Phys.*, 2007, **40**, R319–R336.
42 A. J. Engler, S. Sen, H. L. Sweeney and D. E. Discher, *Cell*, 2006, **126**, 677–689.
43 C. W. Visser, T. Kamperman, L. P. Karbaat, D. Lohse and M. Karperien, *Sci. Adv.*, 2018, **4**, eaao1175.
44 D. Lee, K. Lee and C. Cha, *Adv. Biosyst.*, 2018, **2**, 1800236.
45 J. Folkman, *N. Engl. J. Med.*, 1971, **285**, 1182–1186.
46 R. S. Kerbel, *N. Engl. J. Med.*, 2008, **358**, 2039–2049.
47 M. E. Kaighn, K. S. Narayan, Y. Ohnuki, J. F. Lechner and L. W. Jones, *Invest. Urol.*, 1979, **17**, 16–23.
48 K. Hoyt, B. Castaneda, M. Zhang, P. Nigwekar, P. A. di Sant'Agnese, J. V. Joseph, J. Strang, D. J. Rubens and K. J. Parker, *Cancer Biomarkers*, 2008, **4**, 213–225.
49 J. R. Weis, B. Sun and G. M. Rodgers, *Thromb. Res.*, 1991, **61**, 171–173.
50 J. Oswald, S. Boxberger, B. Jørgensen, S. Feldmann, G. Ehninger, M. Bornhäuser and C. Werner, *Stem Cells*, 2004, **22**, 377–384.
51 R. Janvier, A. Sourla, M. Koutsilieris and C. J. Doillon, *Anticancer Res.*, 1997, **17**, 1551–1557.

52 L. C. Roudsari, S. E. Jeffs, A. S. Witt, B. J. Gill and J. L. West, *Sci. Rep.*, 2016, **6**, 32726.
53 N. Peela, F. S. Sam, W. Christenson, D. Truong, A. W. Watson, G. Mouneimne, R. Ros and M. Nikkhah, *Biomaterials*, 2016, **81**, 72–83.
54 S. P. Singh, M. P. Schwartz, E. Y. Tokuda, Y. Luo, R. E. Rogers, M. Fujita, N. G. Ahn and K. S. Anseth, *Sci. Rep.*, 2015, **5**, 17814.
55 A. Nyga, M. Loizidou, M. Emberton and U. Cheema, *Acta Biomater.*, 2013, **9**, 7917–7926.